

# Monte-Carlo simulation of a thick lens IOL power calculation

Achim Langenbacher<sup>1</sup> | Nóra Szentmáry<sup>2,3</sup> | Alan Cayless<sup>4</sup> | Damien Gatinel<sup>5</sup> | Guillaume Debellemanni<sup>5</sup> | Jascha Wendelstein<sup>1,6,7</sup> | Peter Hoffmann<sup>8</sup>

<sup>1</sup>Department of Experimental Ophthalmology, Saarland University, Homburg/Saar, Germany

<sup>2</sup>Dr. Rolf M. Schwiete Center for Limbal Stem Cell and Aniridia Research, Saarland University, Homburg/Saar, Germany

<sup>3</sup>Department of Ophthalmology, Semmelweis-University, Budapest, Hungary

<sup>4</sup>School of Physical Sciences, The Open University, Milton Keynes, UK

<sup>5</sup>Rothschild Foundation Hospital, Paris, France

<sup>6</sup>Institut für Refraktive- und Ophthalmochirurgie (IROC), Zurich, Switzerland

<sup>7</sup>Department of Ophthalmology, Johannes Kepler University Linz, Linz, Austria

<sup>8</sup>Augen- und Laserklinik Castrop-Rauxel, Castrop-Rauxel, Germany

## Correspondence

Achim Langenbacher, Department of Experimental Ophthalmology, Saarland University, Kirrberger Str 100 Bldg. 22, 66424 Homburg, Germany.  
Email: [achim.langenbacher@uks.eu](mailto:achim.langenbacher@uks.eu)

## Abstract

**Background:** The purpose of this Monte-Carlo study is to investigate the effect of using a thick lens model instead of a thin lens model for the intraocular lens (IOL) on the resulting refraction at the spectacle plane and on the ocular magnification based on a large clinical data set.

**Methods:** A pseudophakic model eye with a thin spectacle correction, a thick cornea (curvatures for both surfaces and central thickness) and a thick IOL (equivalent power PL derived from a thin lens IOL, Coddington factor CL (uniformly distributed from  $-1.0$  to  $1.0$ ), either preset central thickness  $LT=0.9$  mm (A) or optic edge thickness  $ET=0.2$  mm, (B)) was set up. Calculations were performed on a clinical data set containing 21 108 biometric measurements of a cataractous population based on linear Gaussian optics to derive spectacle refraction and ocular magnification using the thin and thick lens IOL models.

**Results:** A prediction model (restricted to linear terms without interactions) was derived based on the relevant parameters identified with a stepwise linear regression approach to provide a simple method for estimating the change in spectacle refraction and ocular magnification where a thick lens IOL is used instead of a thin lens IOL. The change in spectacle refraction using a thick lens IOL with (A) or (B) instead of a thin lens IOL with identical power was within limits of around  $\pm 1.5$  dpt when the thick lens IOL was placed with its haptic plane at the plane of the thin lens IOL. In contrast, the change in ocular magnification from considering the IOL as a thick lens instead of a thin lens was small and not clinically significant.

**Conclusion:** This Monte-Carlo simulation shows the impact of using a thick lens model IOL with preset LT or ET on the resulting spherical equivalent refraction and ocular magnification. If IOL manufacturers would provide all relevant data on IOL design data and refractive index for all power steps, this would make it possible to perform direct calculations of refraction and ocular magnification.

## KEYWORDS

5 surface pseudophakic model eye, linear Gaussian optics, Monte-Carlo simulation, ocular magnification, spherical equivalent refraction, thick lens cornea, thick lens IOL model, vergence calculation

## 1 | INTRODUCTION

After establishing ultrasound biometry as a routine measurement before cataract surgery in clinical practice in the sixties of the last century, the first intraocular lens (IOL) power calculation formulae were introduced by Fyodorov in 1967 (Fyodorov et al., 1975) and by Gernet in 1970 (Gernet et al., 1970). Both formulae are based on paraxial optics and a pseudophakic model eye containing 3 refractive surfaces (intended spectacle refraction (SEQ) after cataract surgery, cornea and IOL) and a fixed axial position of the IOL

implant in the eye. In the following decades, many attempts were made to enhance the formula predicted IOL power and the refraction. The launch of the first optical biometer (IOLMaster) in 1999 can be interpreted as a quantum leap towards better prediction of the post-cataract results, initialising a race between more accurate biometers, more advanced IOL power calculation strategies and optimised IOL designs and manufacturing processes, with the overall goal of minimising the refractive prediction error as the deviation of the achieved from the intended refraction (Fişuş et al., 2021). Nowadays, many empirical (regression or AI

This is an open access article under the terms of the [Creative Commons Attribution](https://creativecommons.org/licenses/by/4.0/) License, which permits use, distribution and reproduction in any medium, provided the original work is properly cited.

© 2023 The Authors. *Acta Ophthalmologica* published by John Wiley & Sons Ltd on behalf of Acta Ophthalmologica Scandinavica Foundation.

based) calculation schemes have been developed (Sanders et al., 1990; Savini et al., 2020; Shammas, 2004), along with theoretical optical formulae based on a pseudophakic model eye containing 3 (Haigis et al., 2000; Hoffer, 1993; Holladay et al., 1988; Retzlaff et al., 1990) or 4 refractive surfaces. Other approaches include numerical raytracing strategies, which use the tomographic measurements of the cornea together with the IOL design data to derive the appropriate lens power and predict the imaging performance of the pseudophakic eye (e.g. Okulix or PhakoOptics software). For example, the Olsen formula (Olsen, 2007; Olsen et al., 1995), or the Castrop formula (Langenbucher et al., 2021; Wendelstein et al., 2022) already make use of measurement data of the corneal front and back surface curvature to enhance the predictability of the postoperative outcome and to avoid the risk of misinterpretation of corneal power in patients with a history of corneal refractive surgery.

Currently, the factor limiting the upgrade of paraxial lens power calculation concepts to a thick lens model for the cornea and the IOL is the lack of design data of the IOLs (Debellemanière et al., 2021; Langenbucher, Hoffmann, et al., 2022). Some IOL designs are published in IP documents (mostly for 1 specific lens power values), but in order to establish such a thick lens IOL power calculation formula the design data have to be known for all power steps of a lens. The IOL Power Club (<https://www.iOLpowerclub.org>) has recently started an initiative to motivate IOL manufacturers to disclose the basic design specifications of their IOLs in order to allow a more precise lens power calculation based on a thick lens model not only for the cornea but also for the lens (Olsen et al., 2023). For low-power lenses, the central thickness of the IOL is small and both radii of curvature are large, which means that dealing with a thin or thick lens model of the IOL is not appreciably different (Langenbucher, Hoffmann, et al., 2022). However, the central thickness of the IOL is not negligible for normal or large lens power values, and the refractive properties of the lens in the eye are poorly reflected by the IOL power alone (Simpson, 2021). Instead, we have to deal with the curvatures or power values of both lens surfaces or alternatively with the equivalent power and the Coddington shape factor, the central thickness of the IOL and the refractive index of the lens optic material, in order to represent the refraction of the lens in the pseudophakic eye accurately. In this context, the Coddington shape factor describes the bending of the IOL, where, for example a value of  $-1$  or  $1$  refers to a plano-convex or convex-plano design, values in the interval between  $-1$  and  $1$  refer to a bi-convex design, and values  $<-1$  or  $>1$  refer to a convex-concave or concave-convex meniscus shaped lens design (Gatinel et al., 2021; Langenbucher, Hoffmann, et al., 2022).

As the shape of an IOL model may vary between all the available power steps, the strategy of lens power calculation based on a thick lens model changes slightly: with a thin lens model for the IOL (with either a thin or thick lens model for the cornea), we can directly calculate the power of the IOL and the predicted postoperative spectacle refraction. However, with a thick lens model of the IOL, the basic optical design of each individual power step has to be considered together with the equivalent power of the

lens as labelled on the package, in order to find the proper lens power promising a residual refraction close to our intended target refraction. We could either roughly estimate the lens power using a thin lens model for the IOL in a first step and in a second step predict the spectacle refraction for several lens powers close to the power of the thin lens derived in the first step. Alternatively, the spectacle refraction could be derived for all available lens powers considering the respective shape data, and the refraction which is most appropriate for the patient defines the IOL power to be used.

Before performing clinical studies focusing on the impact of predictors on the target parameter, a more general Monte-Carlo simulation could help to estimate the effect of the IOL shape and thickness on the predicted refraction comparing a thin and thick lens model for the IOL. In a Monte-Carlo simulation, either 'synthetic data' based on distributions and interactions of clinical measures derived from the literature, or real measurement data from a representative study population, could be used to calculate the effect of IOL shape on the refractive outcome after cataract surgery, and to evaluate the differences between a thin and a thick lens model for the IOL. Monte-Carlo simulations are also quite commonly used for a subsequent linear or nonlinear modelling of the predictor effects based on a regression analysis.

The purpose of the present study is:

- to implement and to use a vergence-based calculation scheme based on linear Gaussian optics (restricted to the paraxial space) and a pseudophakic model eye containing 5 refractive surfaces to set up a Monte-Carlo simulation to investigate the effect of preoperative biometric measurements and IOL shape data and to predict spectacle refraction and ocular magnification,
- to derive the change in spectacle refraction and ocular magnification from using a simple thin lens model for the IOL to a thick lens model for the IOL, to show the results based on a large data set of a population with age-related cataract measured with a modern optical biometer and
- to set up a multilinear prediction model to describe the change in spectacle refraction and ocular magnification from using a simple thin lens model for the IOL to a thick lens model for the IOL.

## 2 | MATERIALS AND METHODS

### 2.1 | Preoperative biometric measures and schematic model eye

Preoperative measurements as derived from a modern optical biometer (IOLMaster 700, Carl-Zeiss-Meditec, Jena, Germany) include: the mean corneal front ( $RC_a$ ) and back surface radii of curvature ( $RC_p$ ), axial length measured from corneal front apex to the retina (AL), central corneal thickness measured from epithelium to endothelium (CCT), anterior chamber depth ( $ACD_{pre}$ ) measured from the corneal epithelium to the front apex of the crystalline lens and the central thickness of the crystalline lens ( $LT_{pre}$ ). As all distances in the eye sum

to AL, the vitreous depth is assumed to be  $AL - ACD_{pre} - LT_{pre}$ . In this context, as a simplification the retinal thickness has been disregarded in our model. Parameters indexed with  $(\ )_{pre}$  ( $ACD_{pre}$  and  $LT_{pre}$ ) are subject to change from the phakic to the pseudophakic eye ( $ACD$  and  $LT$ , respectively), whereas all non-indexed parameters are assumed to remain unchanged. In total, a data set containing 35422 measurements from a cataractous population taken with the IOLMaster 700 was considered in this retrospective data analysis. Incomplete data or data with an insufficient quality mark from the biometer were discarded before further analysis.

All calculations are based on a pseudophakic model eye as shown in Figure 1. This model eye contains 5 refractive surfaces: a thin lens spectacle correction (refractive power: SEQ) at a distance  $VD=12.0\text{mm}$  in front of the corneal apex, a cornea considered as a thick lens and an IOL considered as a thick lens (Gatinel et al., 2021; Langenbucher, Hoffmann, et al., 2022). The thick lens cornea is specified by curvatures  $RC_a$  and  $RC_p$  at the front and back surface, a central thickness  $CCT$  and a refractive index  $nC$ . The thick lens IOL is specified by its equivalent power (PL, paraxial power according to the Gullstrand formula), its Coddington shape factor (CL), its refractive index  $nL$ , and either its central thickness (LT) or its edge thickness (ET), together with the optical diameter (LD). The corresponding calculation scheme for LT or ET from the IOL refractive index and either the radii of the front and back surface or PL and CL is described in another paper (Langenbucher, Hoffmann, et al., 2022). In a previous study, the axial position of the equatorial plane of the crystalline lens (EP) was reported to be located at  $EP=0.0393 \cdot AL + 0.7549 \cdot ACD_{pre} + 0.3823 \cdot LT_{pre}$  behind the corneal front vertex (coefficient of determination  $R^2=0.70$ , root-mean-squared prediction error 0.189mm, Langenbucher, Szentmáry, et al., 2022c). For our model, we assumed that the thin lens IOL as well as

the haptic plane of the thick lens IOL (defined by the centre plane of the optic edge) both match the EP of the phakic eye. From  $RC_a$ ,  $RC_p$ ,  $CCT$  and  $nC$ , we calculated the ratio of back to front surface curvature  $RC_p/RC_a$  and the location of the corneal image-side principal plane (HC).

The data processing included the following steps:

- Initialisation: The refractive index of the cornea ( $nC=1.376$ ), aqueous humour ( $nA=1.336$ ), and vitreous ( $nV=1.336$ ) are extracted from a schematic model eye (Liou & Brennan, 1997). The intended target refraction of the pseudophakic eye at the spectacle plane (TR) was assumed to be randomly distributed in a range between  $-0.25$  and  $0.00$  dpt (uniform distribution). The Coddington factor CL for the thick lens IOL model was assumed to be randomly distributed in an interval from  $CL=-1$  (plano-convex) to  $CL=1$  (convex-plano).
- The refractive power of a thin lens IOL (PL) located at an axial position EP behind the corneal front apex was derived to correct the eye for the intended spectacle correction  $SEQ_{thin}=TR$ . From the product of all vergences before all refractive surfaces and the product of all vergences behind all refractive surfaces the ocular magnification for the spectacle-corrected pseudophakic eye (Langenbucher, Szentmáry, et al., 2022b) with the thin lens IOL ( $OM_{thin}$ ) was predicted.
- From the equivalent power of the thin lens IOL derived in the previous step (PL), the Coddington factor CL, and the refractive index  $nL$  (preset to  $nL=1.52$  without loss of generality), the shape of the thick lens IOL was calculated and the haptic plane EP (EP-ACD behind the IOL front apex) and the image-side principal plane (HL, HL-ACD behind the IOL front apex) was derived. Two different situations were considered: situation 1 refers to a predefined lens thickness LT

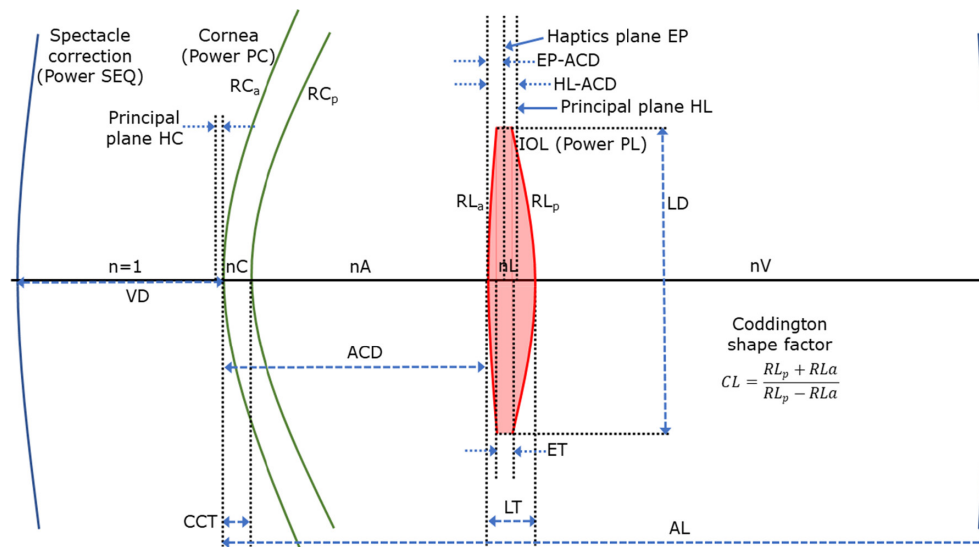


**FIGURE 1** Schematic drawing of the pseudophakic model eye containing 5 refractive surfaces: a spectacle correction, a thick lens cornea defined by front and back surface curvatures  $RC_a$  and  $RC_p$  and a central thickness  $CCT$ , and a thick lens IOL (front and back surface curvatures  $RL_a$  and  $RL_p$ ) defined by an equivalent power PL, a Coddington shape factor CL, either a central lens thickness LT or an edge thickness ET together with optical diameter LD. EP refers to the haptic plane of the IOL (= equator plane of the crystalline lens), and HC and HL to the image-side principal planes of the cornea and IOL.  $nC$ ,  $nA$ ,  $nL$  and  $nV$  refer to the refractive indices of the cornea, aqueous, IOL and vitreous respectively, and  $VD$ ,  $ACD$  to the vertex distance and the pseudophakic anterior chamber depth (defined as the distance from corneal epithelium to the lens front apex).

(with variation of edge thickness ET), and situation 2 to a predefined optic edge thickness ET (calculated from both the curvatures of the IOL and the optical diameter LD, with variation of lens thickness LT).

- The volume of the lens optic part (LVOL) was considered as the sum of the volumes of the anterior part of the lens (positive value for  $CL > -1$  and 0 for a convex-plano lens with  $CL = -1$ ), of the posterior part of the lens (positive value for  $CL < 1$  and 0 for a convex-plano lens with  $CL = 1$ ) and the cylindrical part with thickness ET and diameter LD.
- The thick lens model IOL (with an equivalent power PL derived from the thin lens model in the previous step) was placed with its haptic plane EP at the equatorial plane of the crystalline lens, and the spherical equivalent refraction at the spectacle plane ( $SEQ_{\text{thick}}$ ) was extracted. In addition, from the product of all vergences before all refractive surfaces and the product of all vergences behind all refractive surfaces the ocular magnification for the spectacle-corrected pseudophakic eye (Langenbucher, Szentmáry, et al., 2022b) with the thick lens IOL ( $OM_{\text{thick}}$ ) was predicted.

## 2.2 | Monte-Carlo simulation and data analysis

For the entire data set, the distributions of the EP and the HL with respect to the lens front apex as well as the relative position of HL with respect to EP were calculated for both situations (1: predefined LT and 2: predefined ET). In addition, for situation 1 the distribution of ET and for situation 2 the distribution of LT was assessed. Then, the differences in predicted spherical equivalent at the spectacle plane for the thick lens and thin lens model of the IOL ( $SEQ_{\text{thick}} - SEQ_{\text{thin}}$ ) and the ocular magnification differences for the thick lens and thin lens model of the IOL ( $OM_{\text{thick}} - OM_{\text{thin}}$ ) were derived.

These differences ( $SEQ_{\text{thick}} - SEQ_{\text{thin}}$  and  $OM_{\text{thick}} - OM_{\text{thin}}$ ) were modelled in a multivariable linear model to assist clinicians with a simplified prediction of the effect of considering a thick lens IOL instead of a thin lens IOL. The relevant parameters for this prediction model were identified using a stepwise regression algorithm starting from a constant model. For simplicity, we restricted the analysis to a linear model without interaction terms between parameters.  $RC_a$ ,  $RC_p$ ,  $RC_p/RC_a$ , CCT, AL,  $ACD_{\text{pre}}$ ,  $LT_{\text{pre}}$ ,  $SEQ_{\text{thin}}$ , PL, CL and ET (situation 1) or LT (situation 2) were considered as potential predictors for the model. The stepwise regression refers to a method for adding terms to or removing terms from a multilinear model based on their significance. Starting from the initial (constant) model, the model successively adds predictors where the significance level is smaller than 0.05 and/or removes predictors where the significance level is larger equal 0.05. In each step the predictor with the smallest significance level is considered for being added to the model. A least squares fit is used to estimate the model coefficients in each iteration.

For explorative data analysis the mean, standard deviation, median and the 95% confidence interval (with the 2.5% quantile as the lower boundary and the 97.5% quantile as the upper boundary) were considered. Due to

lack of normal distributions for some of the parameters, the Spearman rank correlation coefficient R was used to specify correlations between scale parameters.

## 3 | RESULTS

For this retrospective analysis, a total of  $N=35422$  biometric measurements from a cataractous population were transferred to our institute in an anonymised fashion (anonymised at the source). Measurements were carried out at Augenklinik Castrop-Rauxel ( $N=24533$ ) and Department of Ophthalmology and Optometry, Johannes Kepler University Linz ( $N=10889$ ). Out of the total of  $N=35422$  biometric measurements,  $N=21\,108$  measurements (21 108 eyes of 21 108 patients; 11 822 female and 9284 male patients; mean age  $68.89 \pm 12.21$  years) were finally included after discarding measurements with incomplete data, duplicate measurements of eyes, or insufficient quality check of the biometer. In cases where measurements of both eyes were available, one eye per patient was randomly selected and included in our data set. Ultimately, 10 653 left and 10 455 right eyes were considered. The local ethics committee provided a waiver for this retrospective data analysis (Ärztammer des Saarlandes, registration number 157/21).

The relevant characteristics of our data set used for analysis are listed in Table 1 showing the mean, standard deviation and median, plus the lower and upper boundaries of the 95% confidence interval of the input parameters  $RC_a$ ,  $RC_p$ ,  $RC_p/RC_a$ , PC, AL, CCT,  $ACD_{\text{pre}}$ ,  $LT_{\text{pre}}$ . Table 2a lists the mean, standard deviation, median and the lower and upper boundaries of the 95% confidence interval of the general lens-associated parameters: the lens equatorial plane position EP calculated from the axial length AL, the phakic anterior chamber depth  $ACD_{\text{pre}}$ , and the phakic lens thickness  $LT_{\text{pre}}$ , the equivalent power of the thin lens model IOL PL, the Coddington shape factor (assumed to be uniformly distributed between  $-1.0$  and  $1.0$ ), the spherical equivalent refraction at the spectacle plane (intended target refraction) considered for the thin lens model of the IOL (assumed to be uniformly distributed in a range  $-0.25 \dots 0.0$  dpt), as well as the ocular magnification of the eye based on the thin lens model for the IOL. Table 2b shows the mean, standard deviation, median and the lower and upper boundaries of the 95% confidence interval for the output data with the IOL thickness preset to  $LT=0.9$  mm (situation 1, edge thickness ET is derived from the lens shape data) or with the IOL optic edge thickness preset to  $ET=0.2$  mm (situation 2, lens thickness LT is derived from the lens shape data). This table includes the IOL front and back surface powers  $PL_a$  and  $PL_p$ , the ET for situation 1 or LT for situation 2, the volume of the lens optic, the locations of the equator plane and the image-side principal plane of the IOL relative to the anterior apex (EP-ACD and HL-ACD), the relative position of the principal plane relative to the haptic plane (HL-EP), the spherical equivalent refraction and ocular magnification if the IOL is considered as thick lens model ( $SEQ_{\text{thick}}$  and  $OM_{\text{thick}}$ ), and the change in spherical equivalent and ocular magnification if the IOL is considered as thick lens instead of thin lens ( $SEQ_{\text{thick}} - SEQ_{\text{thin}}$  and  $OM_{\text{thick}} - OM_{\text{thin}}$ ).

**TABLE 1** Mean, standard deviation, median and the lower and upper boundaries of the 95% confidence interval of the relevant data used for the analysis:  $RC_a$  and  $RC_p$  refer to the radii of curvature of the corneal front and back surface, PC to the equivalent power of the cornea, HC to the location of the image-side principal plane of the cornea, AL to the axial length, CCT to the central corneal thickness and  $ACD_{pre}$  and  $LT_{pre}$  to the anterior chamber depth measured from the corneal front apex to the lens front apex and the central lens thickness of the phakic eye.

| $N=21.108$         | $RC_a$ in mm | $RC_p$ in mm | $RC_p/RC_a$ | PC in dpt | HC in mm | AL in mm | CCT in mm | $ACD_{pre}$ in mm | $LT_{pre}$ in mm |
|--------------------|--------------|--------------|-------------|-----------|----------|----------|-----------|-------------------|------------------|
| Mean               | 7.710        | 6.870        | 0.891       | 43.109    | -0.055   | 23.624   | 0.552     | 3.128             | 4.628            |
| Standard deviation | 0.273        | 0.283        | 0.018       | 1.530     | 0.004    | 1.227    | 0.0370    | 0.380             | 0.406            |
| Median             | 7.706        | 6.865        | 0.891       | 43.077    | -0.055   | 23.474   | 0.551     | 3.124             | 4.643            |
| 2.5% quantile      | 7.199        | 6.340        | 0.856       | 40.187    | -0.064   | 21.590   | 0.482     | 2.399             | 3.477            |
| 97.5% quantile     | 8.258        | 7.438        | 0.924       | 46.118    | -0.047   | 26.641   | 0.627     | 3.886             | 5.356            |

**TABLE 2A** Mean, standard deviation, median and the lower and upper boundaries of the 95% confidence interval of the relevant simulation data (common data for situations 1 and 2): The equator plane of the crystalline lens EP is calculated from AL,  $ACD_{pre}$  and  $LT_{pre}$  and is assumed to coincide with the haptic plane of the IOL in the pseudophakic eye, PL refers to the IOL power derived from the thin lens model (also used as equivalent power for the thick lens model), CL to the Coddington shape factor which is uniformly distributed between -1.0 and 1.0,  $SEQ_{thin}$  to the intended spherical equivalent refraction of the pseudophakic eye for the thin lens model of the IOL (uniformly distributed between -0.25 and 0.00 dpt), and  $OM_{thin}$  to the ocular magnification of the spectacle-corrected phakic eye for the thin lens model of the IOL.

| $N=21.108$         | EP in mm | PL in dpt | CL     | $SEQ_{thin}$ in dpt | OMthin in mm/<br>mrad (x1000) |
|--------------------|----------|-----------|--------|---------------------|-------------------------------|
| Mean               | 5.959    | 20.733    | -0.000 | -0.125              | 16.611                        |
| Standard deviation | 0.254    | 3.948     | 0.578  | 0.072               | 1.021                         |
| Median             | 5.052    | 21.283    | 0.002  | -0.125              | 16.466                        |
| 2.5% quantile      | 4.576    | 10.879    | -0.946 | -0.243              | 14.959                        |
| 97.5% quantile     | 5.573    | 27.555    | 0.955  | -0.006              | 19.213                        |

Figure 2 displays for situation 1 (left graph) and situation 2 (right graph) the (distributions of the) IOL haptic plane EP and image-side principal plane HL relative to the front apex plane (upper graphs, origin of the x-axis), the distribution of the edge thickness ET and the lens

We subsequently used a stepwise linear regression approach to identify the relevant input parameters in order to properly describe the output parameters  $SEQ_{thick}$ ,  $SEQ_{thin}$  and  $OM_{thick}-OM_{thin}$  for situations 1 and 2. Finally, the linear prediction models for situation 1 with a preset lens thickness  $LT=0.9$  mm are:

$$\begin{aligned} SEQ_{thick} - SEQ_{thin} &= -3.4656 - 0.0772 \cdot RC_a + 0.1130 \cdot PL - 0.8990 \cdot CL + 4.1720 \cdot ET + 0.0151 \cdot AL - 0.0005 \cdot ACD_{pre} \\ OM_{thick} - OM_{thin} &= 10^{-4} \cdot (-0.6495 + 0.0246 \cdot PL - 0.7329 \cdot CL + 0.8537 \cdot ET - 0.0286 \cdot SEQ_{thin} - 0.0171 \cdot AL) \end{aligned}$$

thickness LT relative to the front apex plane (middle graphs, origin of the x-axis), and the distributions of the location of the image-side principal plane HL relative to the haptic plane EP (HL-EP) for situation 1 (lower left image) and situation 2 (lower right image).

The root-mean-squared fit error of the linear model  $0.1472/1.2128 \cdot 10^{-5}$  (F-value  $4.0681 \cdot 10^4$   $4.7815 \cdot 10^4$ ) for  $SEQ_{thick}-SEQ_{thin}/OM_{thick}-OM_{thin}$  model, respectively, and the significance level was  $<10^{-5}$  for both models.

The linear prediction models for situation 2 with a preset optic edge thickness  $ET=0.2$  mm are:

$$\begin{aligned} SEQ_{thick} - SEQ_{thin} &= 0.6554 - 0.1002 \cdot RC_a + 0.1108 \cdot PL - 0.8035 \cdot CL - 3.5373 \cdot LT + 0.0299 \cdot AL - 0.0127 \cdot ACD_{pre} \\ OM_{thick} - OM_{thin} &= 10^{-4} \cdot (0.0988 - 0.0377 \cdot RC_a - 0.6551 \cdot PL + 0.0031 \cdot AL) \end{aligned}$$

Figure 3 shows the correlation plots for situation 1 (Figure 3a) and situation 2 (Figure 3b) analysing the impact of the potential input parameters  $RC_a$ ,  $RC_p/RC_a$ , CL, ET (situation 1) or LT (situation 2),  $SEQ_{thin}$ , AL, and  $ACD_{pre}$  on the output parameters of our linear prediction model of the change in spherical equivalent refraction ( $SEQ_{thick}-SEQ_{thin}$  and  $OM_{thick}-OM_{thin}$ ) if the IOL is considered as thick lens model instead of a thin lens model. These graphs imply that there is an excellent inter-correlation between both output parameters  $SEQ_{thick}-SEQ_{thin}$  and  $OM_{thick}-OM_{thin}$  and an inverse correlation of both output parameters to the Coddington shape factor CL of the IOL. The Spearman rank correlation coefficients are shown as numbers in the subplots.

The root-mean-squared fit error of the linear model  $0.1633/1.3352 \cdot 10^{-5}$  (F-value  $2.6434 \cdot 10^4$   $5.2372 \cdot 10^4$ ) for  $SEQ_{thick}-SEQ_{thin}/OM_{thick}-OM_{thin}$  model, respectively, and the significance level was  $<10^{-5}$  for both models.

Figure 4 displays the prediction model performance scatter/histogram plots (scatterplots with marginal probability density distribution graphs) in terms of predicted output parameters (y-axis) versus observed output parameters (x-axis) for the change in spherical equivalent refraction at the spectacle plane ( $SEQ_{thick}-SEQ_{thin}$ , Figure 4a) and ocular magnification ( $OM_{thick}-OM_{thin}$ , Figure 4b) using a thick lens model for the IOL instead of a thin lens model. In both scatter/histogram graphs, the blue/red dots refer to the prediction model with situation

**TABLE 2B** Mean, standard deviation, median and the lower and upper boundaries of the 95% confidence interval of the relevant data used for the analysis (for situations 1 and 2):  $PL_a$  and  $PL_p$  refer to the surface power of the IOL front and back surface,  $LT/ET$  to the edge thickness (situation 1 with preset  $LT$ ) or the lens thickness (situation 2 with preset edge thickness),  $LVOL$  to the volume of the lens optics part,  $EP-ACD$  and  $HL-ACD$  to the positions of the equator and image-side haptic planes with respect to the IOL front apex,  $HL-EP$  to the position of the principal plane relative to the haptic plane,  $SEQ_{thick}$  and  $OM_{thick}$  to the spherical equivalent refraction at the spectacle plane and ocular magnification based on the thick lens model, and  $SEQ_{thick}-SEQ_{thin}$  and  $OM_{thick}-OM_{thin}$  to the change in spherical equivalent refraction and ocular magnification if the IOL is considered as a thick lens model instead of a thin lens model.

| $N=21.108$                      |                    | $PL_a$ in dpt | $PL_p$ in dpt | $LT/ET$ in mm | $LVOL$ in $mm^3$ | $EP-ACD$ in mm | $HL-ACD$ in mm | $HL-EP$ in mm | $SEQ_{thick}$ in dpt | $SEQ_{thick}-SEQ_{thin}$ in dpt | $OM_{thick}$ in mm/mrad ( $\times 1000$ ) | $OM_{thick}-OM_{thin}$ in mm/mrad ( $\times 1000$ ) |
|---------------------------------|--------------------|---------------|---------------|---------------|------------------|----------------|----------------|---------------|----------------------|---------------------------------|---|---|
| Situation 1: preset $LT=0.9$ mm | Mean               | 10.405        | 10.370        | 0.384         | 18.185           | 0.451          | 0.504          | 0.053         | 0.088                | 0.213                           | 16.590                                    | -0.021  |
|                                 | Standard deviation | 6.437         | 6.355         | 0.101         | 1.407            | 0.153          | 0.229          | 0.380         | 0.545                | 0.541                           | 1.020                                     | 0.044   |
|                                 | Median             | 9.983         | 9.99          | 0.370         | 17.998           | 0.450          | 0.503          | 0.052         | 0.092                | 0.212                           | 16.449                                    | -0.023  |
|                                 | 2.5% quantile      | 0.523         | 0.430         | 0.207         | 15.740           | 0.187          | 0.127          | -0.583        | -0.912               | -0.772                          | 14.931                                    | -0.098  |
|                                 | 97.5% quantile     | 22.612        | 22.338        | 0.632         | 21.668           | 0.719          | 0.879          | 0.679         | 1.065                | 1.184                           | 19.185                                    | 0.062   |
| Situation 2: preset $ET=0.2$ mm | Mean               | 10.400        | 10.373        | 0.716         | 12.996           | 0.359          | 0.401          | 0.042         | 0.046                | 0.171                           | 16.594                                    | -0.017  |
|                                 | Standard deviation | 6.432         | 6.355         | 0.101         | 1.446            | 0.163          | 0.191          | 0.337         | 0.498                | 0.493                           | 1.021                                     | 0.040   |
|                                 | Median             | 9.979         | 9.989         | 0.729         | 13.177           | 0.346          | 0.391          | 0.040         | 0.037                | 0.157                           | 16.452                                    | -0.017  |
|                                 | 2.5% quantile      | 0.517         | 0.431         | 0.468         | 9.446            | 0.113          | 0.099          | -0.539        | -0.873               | -0.731                          | 14.937                                    | -0.091  |
|                                 | 97.5% quantile     | 22.593        | 22.368        | 0.892         | 15.516           | 0.673          | 0.757          | 0.622         | 0.986                | 0.105                           | 19.192                                    | 0.059   |

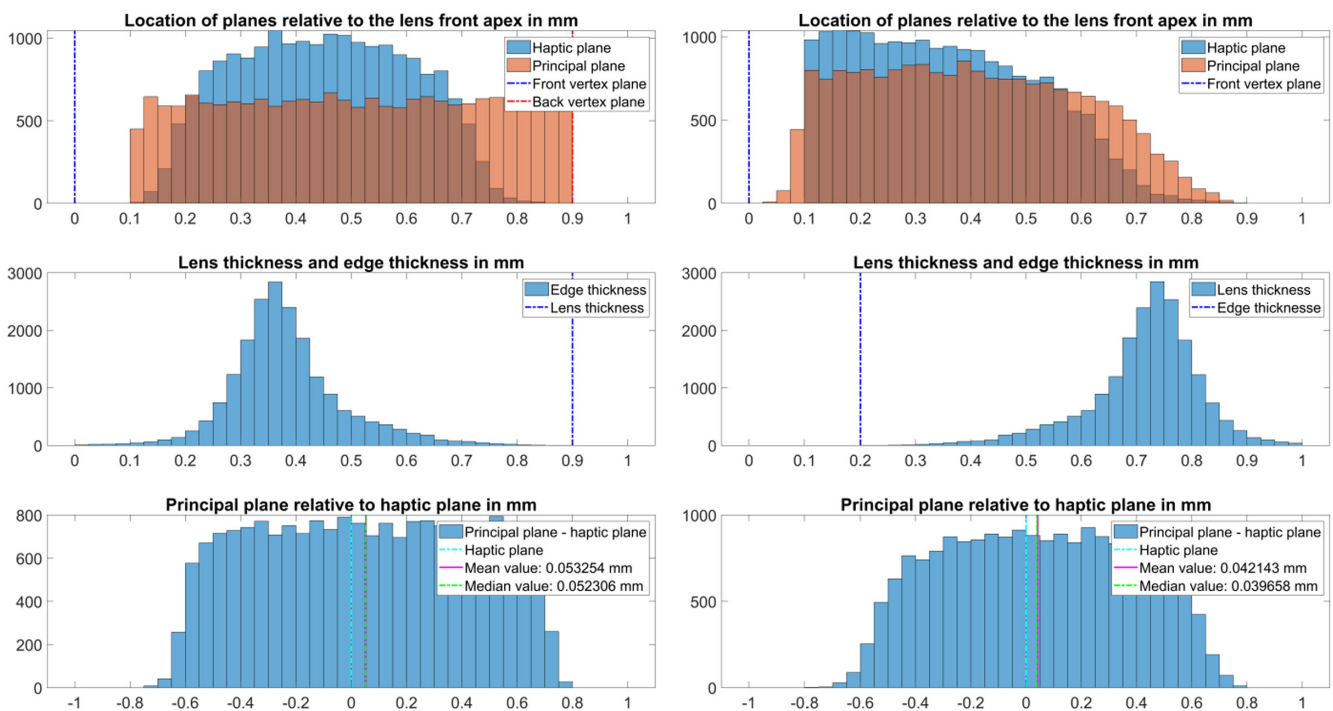
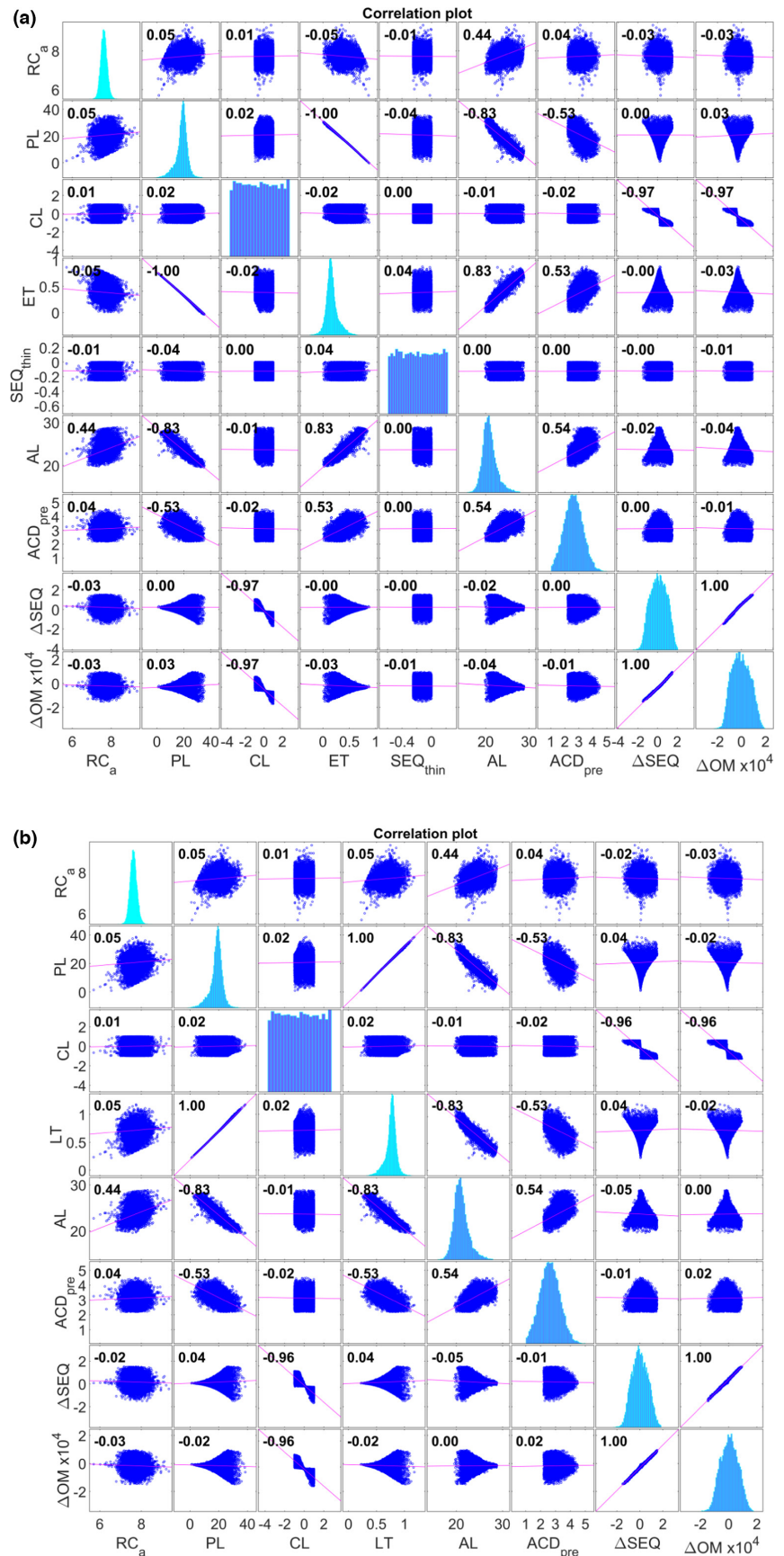


**FIGURE 2** Overview on the distributions of the plane locations for situation 1 (left image; preset lens thickness  $LT=0.9$  mm) and situation 2 (right image; preset optic edge thickness  $ET=0.2$  mm). Upper graphs: distribution of the locations of the haptic plane ( $EP-ACD$ ) and the image-side principal plane ( $HL-ACD$ ) with respect to the IOL front apex. The origin on the x-axis coincides with the IOL front apex plane. Middle graphs: Distribution of the optic edge thickness ( $ET$ , situation 1) and the lens thickness ( $LT$ , situation 2). The origin on the x-axis coincides with the IOL front apex plane, and the blue line indicates the preset lens thickness  $LT$  (left image, situation 1) or the preset edge thickness (right image, situation 2). Lower graphs: Distribution of the image-side principal plane relative to the haptic plane ( $HL-EP$ ). The position of the haptic plane  $EP$  is indicated by the cyan line, and the mean and median offset  $HL-EP$  is indicated with the magenta and green line.

1 (preset lens thickness  $LT=0.9$  mm)/situation 2 (preset optic edge thickness  $ET=0.2$  mm). In both graphs, the scatterplot shows a slight nonlinearity which cannot be fully mapped by the linear prediction model without interaction terms. However, for clinical purposes this simple linear prediction model seems to provide a

reasonable estimate for the changes in spherical equivalent refraction and ocular magnification if a thick lens model is considered for the IOL instead of a thin lens model. The PDF plots below the scatterplots refer to the Kernel distributions of the observed  $SEQ_{thick}-SEQ_{thin}$  and  $OM_{thick}-OM_{thin}$  for situation 1 (blue line)

**FIGURE 3** Correlation plot to identify the relevant parameters for the linear prediction model for the change in spherical equivalent refraction at the spectacle plane in dioptres ( $\Delta\text{SEQ} = \text{SEQ}_{\text{thick}} - \text{SEQ}_{\text{thin}}$ ) and ocular magnification ( $\Delta\text{OM} = \text{OM}_{\text{thick}} - \text{OM}_{\text{thin}}$ ) if a thick lens model (defined with equivalent power PL, Coddington shape factor CL, preset refractive index  $n_L = 1.52$  and preset lens thickness  $LT = 0.9\text{ mm}$  (situation 1, Figure 3a) or optic edge thickness  $ET = 0.2\text{ mm}$  (situation 2, Figure 3b)) is considered for the IOL instead of a thin lens model characterised with a power PL. The input parameters for the linear regression model shown are:  $RC_a$  refers to the corneal front surface radius in mm, PL, CL, ET (situation 1) or LT (situation 2), AL refers to the axial length in mm,  $ACD_{\text{pre}}$  to the anterior chamber depth of the phakic eye in mm, and  $\text{SEQ}_{\text{thin}}$  to the spherical equivalent refraction of the pseudophakic eye in dpt (target refraction) based on a thin lens model for the IOL. Only those predictors included in the final model are shown in the graph. Other potential predictors include:  $RC_p/RC_a$  (ratio of corneal back to front surface radii), CCT (central corneal thickness in mm), and  $LT_{\text{pre}}$  (central thickness of the crystalline lens in mm). In both situations there is a strong correlation between both target parameters ( $\Delta\text{SEQ} = \text{SEQ}_{\text{thick}} - \text{SEQ}_{\text{thin}}$  and  $\Delta\text{OM} = \text{OM}_{\text{thick}} - \text{OM}_{\text{thin}}$ ) and an inverse correlation with the spherical equivalent refraction at the spectacle plane intended for the thin lens model for the IOL.



and situation 2 (red line), and the PDF plot on the left refers to the Kernel distributions of the predicted  $\text{SEQ}_{\text{thick}} - \text{SEQ}_{\text{thin}}$  and  $\text{OM}_{\text{thick}} - \text{OM}_{\text{thin}}$ , respectively. The PDF plots indicate that in our calculation model (with a preset IOL refractive index of  $n_L = 1.52$  and a preset IOL thickness LT or edge thickness ET), by using a thick lens model for

the IOL with the same equivalent power PL as the thin lens model placed with the haptic plane EP at the same position as the thin lens, a variation of the Coddington shape factor in a range between  $-1.0$  and  $1.0$  could effect a difference in spherical equivalent refraction of up to  $\pm 1.5$  dpt compared to the thin lens model for the IOL.

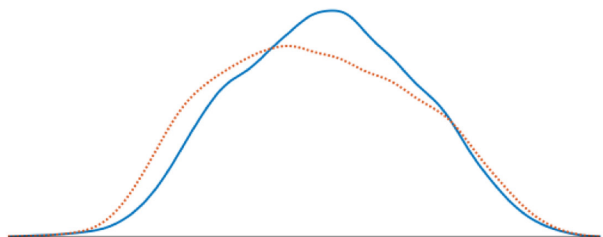
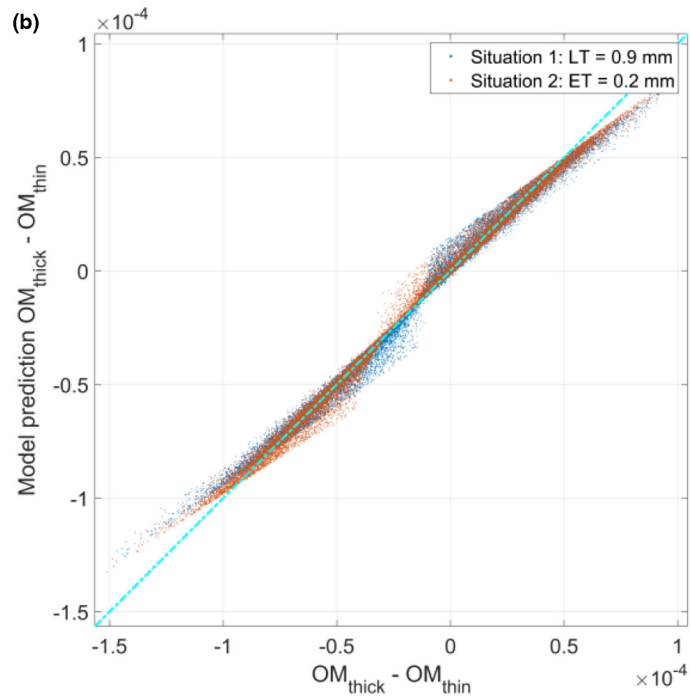
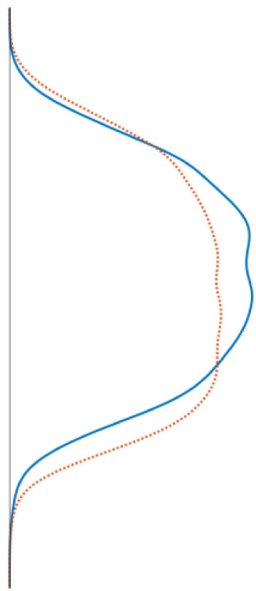
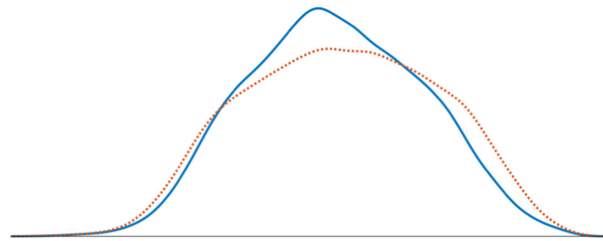
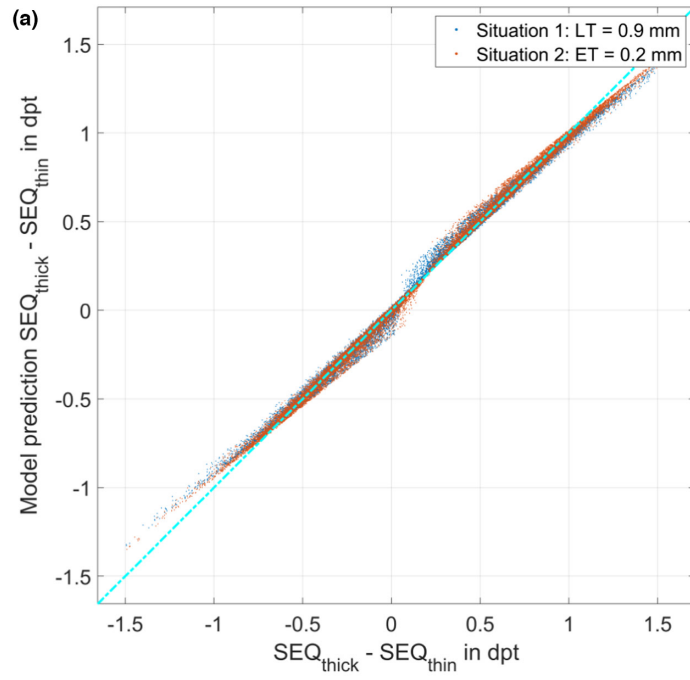
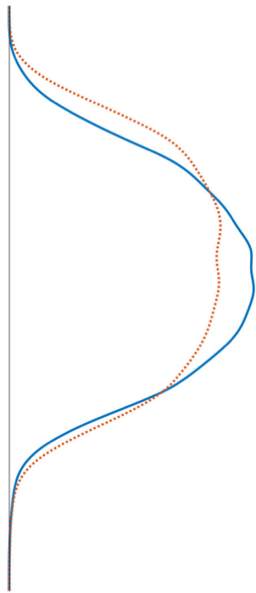


**FIGURE 4** Linear model (modelled value on the y-axis vs. the calculated value on the x-axis) for the change in spherical equivalent refraction at the spectacle plane in dioptres ( $SEQ_{\text{thick}}-SEQ_{\text{thin}}$ , Figure 4a) and ocular magnification ( $OM_{\text{thick}}-OM_{\text{thin}}$ , Figure 4b) if a thick lens model is considered for the IOL instead of a thin lens model. In both scatterhistogram graphs, the blue/red dots refer to the prediction model with situation 1 (preset lens thickness  $LT=0.9\text{mm}$ )/situation 2 (preset optic edge thickness  $ET=0.2\text{mm}$ ). The PDF plots below the scatterplot show the Kernel distributions for the calculated ( $SEQ_{\text{thick}}-SEQ_{\text{thin}}$  and  $OM_{\text{thick}}-OM_{\text{thin}}$ ), and the PDF plots on the left show the Kernel distributions for the linear model output of ( $SEQ_{\text{thick}}-SEQ_{\text{thin}}$  and  $OM_{\text{thick}}-OM_{\text{thin}}$ ), respectively. In this simulation, the IOL refractive index was set to  $nL=1.52$  and the Coddington shape factor  $CL$  was uniformly distributed within the range  $(-1.0..1.0)$ .

## 4 | DISCUSSION

With the latest generation of optical biometers established in the last decade we are able to measure all axial distances in the eye such as axial length, central corneal thickness, aqueous depth, central lens thickness and vitreous depth, together with the curvature of the cornea, all with a very high precision (Fişuş et al., 2021). In most of the instruments a plug-in keratometer or Placido disc topographer is integrated for measurement of corneal curvature, and with the newest scanning optical coherence measurements additional features are available, for example to derive the corneal back surface curvature. All these data could be used for IOL power calculation, even where the classical formulae first published in the 80th and 90th of the last century are restricted to the measurement data available that time, mostly the axial length and corneal front surface curvature (or K readings (Hoffer & Savini, 2021; Melles et al., 2019; Savini et al., 2020)). With modern formulae developed in the last 2 decades the formula prediction error in terms of the deviation of the achieved refraction from the formula predicted refraction considered at the spectacle plane could be reduced significantly. However, up to now the overwhelming majority of IOL power calculation concepts use a single parameter 'equivalent power' PL for the lens to describe the refractive properties. This is mostly due to the lack of published IOL design data.

One remaining drawback which prevents further improvement of IOL power calculation is the restriction to IOLs considered as a thin lens model (Simpson, 2021). Especially in short eyes requiring a high-power IOL the central thickness of the IOL cannot be neglected, and the IOL must be described using the equivalent power PL, the Coddington shape factor CL, the central thickness LT, the asphericity of both IOL surfaces, and the refractive index  $nL$ . As a simplification, especially when dealing with linear Gaussian optics, any asphericity of the IOL surfaces is not taken into account and we restrict the model to the curvatures of both surfaces together with the central thickness and the optic material refractive index instead of using the power of the IOL.

Calculating the eye using a thick lens setup is not only a domain of numerical raytracing (Gatinel et al., 2021; Langenbucher, Hoffmann, et al., 2022), even though raytracing enables consideration of the full shape data including asphericity or prediction of the effect of decentration or tilt of refractive surfaces or the effect of an aperture in the optical pathway. In the current study, we used a large data set with biometric measurements derived from a cataractous population to perform a Monte-Carlo simulation. We used the  $AL$ ,  $CCT$ ,  $ACD_{\text{pre}}$  and  $LT_{\text{pre}}$  of the phakic eye together with the curvature of the corneal front and back surface  $RC_a$  and  $RC_p$  to

calculate all relevant metrics of the pseudophakic eye using a thick lens model for the IOL. The strategy of calculation was as follows: first, we predicted the equator plane of the crystalline lens from the phakic biometric data and placed a thin lens at this plane (Norrby & Koranyi, 1997; Olsen, 2006; Olsen & Hoffmann, 2014). The target refraction at the spectacle plane was assumed to be uniformly distributed between plano and minus  $\frac{1}{4}$  dpt. With the refractive indices of the cornea, aqueous humour and vitreous derived from a schematic model eye (Liou & Brennan, 1997), we calculated the respective IOL lens power PL and the ocular magnification  $OM_{\text{thin}}$  of the spectacle-corrected eye as the ratio of retinal image size to incident ray angle in radians (Harris, 2000; Langenbucher, Szentmáry, et al., 2022b). Then we replaced this thin lens model IOL by a thick lens model IOL defined by the same power (equivalent power PL), a refractive index  $nL$ , and either a preset IOL thickness LT (situation 1) or a preset optic edge thickness ET (situation 2). The Coddington shape factor of this lens was assumed to be uniformly distributed between  $-1.0$  (plano-convex IOL) and  $1.0$  (convex-plano IOL) to map the normal range of bi-convex IOL designs. We then performed calculations on the pseudophakic eye with the thick lens IOL where the haptic plane was again assumed to match the equator plane of the crystalline lens (or the plane of the thin lens IOL). The principal plane of the lens and the volume of the thick lens IOL optic were derived, and the spherical equivalent refraction at spectacle plane  $SEQ_{\text{thick}}$  and the ocular magnification  $OM_{\text{thick}}$  were calculated. As a final step, we set up a linear prediction model (for simplicity by excluding mixed terms) to describe the change in spectacle refraction ( $SEQ_{\text{thick}}-SEQ_{\text{thin}}$ ) and ocular magnification ( $OM_{\text{thick}}-OM_{\text{thin}}$ ) in terms of the potential input parameters from biometry ( $RC_a$  and  $RC_p/RC_a$ ),  $AL$ ,  $CCT$ ,  $ACD_{\text{pre}}$ ,  $LT_{\text{pre}}$ , together with the target refraction  $SEQ_{\text{thin}}$ , the lens power PL, the Coddington factor CL and the IOL thickness LT (situation 1) or optic edge thickness ET (situation 2). A linear stepwise algorithm was used to identify the relevant input parameters of this model by stepwise adding and removing parameters based on their impact on the model (statistical significance level).

The most relevant findings of our study are that based on our model settings, if we use a thick lens model for the IOL instead of a thin lens model the change in spherical equivalent refraction at spectacle plane varies between  $-1.5$  and  $1.5$  dpt (95% confidence interval  $-0.772$  to  $1.1813$  dpt/ $-0.7306$  to  $1.1052$  dpt for situations 1/2), which cannot be neglected in clinical routine. We also found that with a preset LT in situation 1 the thick lens IOL is on average slightly thicker compared to situation 2 with a preset ET and also that the IOL optic volume LVOL is much smaller. To our

understanding this result is not surprising: IOL manufacturers always aim to produce their IOLs as thin as possible, while maintaining a minimum optic edge thickness for assembly of the IOL haptics as assumed in situation 2 with  $ET=0.2\text{ mm}$ . In contrast, if we preset the IOL thickness (situation 1) e.g. to a standard  $LT=0.9\text{ mm}$ , the edge thickness (and the IOL optic volume LVOL) is in most cases unnecessarily large, making insertion of the IOL difficult. The second relevant finding of our study is that the change in ocular magnification when considering the IOL as a thick lens instead of a thin lens is rather small and can be neglected in clinical routine. This means that the options of using the thick IOL as an 'eikonic lens' to adapt the ocular magnification of both eyes by variation of the Coddington shape factor in order to reduce or avoid pseudophakic aniseikonia are limited. Therefore, in clinical practice, aniseikonia treatment during cataract surgery should be performed with proper combinations of target refraction and IOL power. The present study was restricted to Coddington shape factors in a range between  $-1.0$  and  $1.0$ . For very low-power IOLs (e.g.  $<6.0\text{ dpt}$  or  $<0.0\text{ dpt}$  for high myopes) some manufacturers use convex-concave meniscus designs with a shape factor  $<-1$ . With these lenses, the image-side principal plane is no longer located between the IOL front and back apex, and the results could deviate slightly from the results shown in the Results section. However, for these low-power lenses the LT is typically rather low, and the effect of the shape factor on the resulting refraction or ocular magnification is not expected to be clinically relevant.

With the linear prediction models, we wanted to provide clinicians with a simple method of predicting the change of spectacle refraction and ocular magnification where a thick lens IOL is considered instead of a thin lens IOL. The prediction models shown for situations 1 and 2 are simplified by restricting them to a linear model without potential interactions based on the relevant input parameters identified with a stepwise linear regression approach. As shown in Figure 4, the results of this prediction are not perfect, and by including mixed terms (not shown in the Results section) the prediction performance could be significantly improved, but at the cost of the simplicity. We therefore decided to provide the simple linear model instead of the more complex mixed model, in order to enable clinicians to implement this model using standard software tools such as EXCEL.

There are however some limitations of our study, mostly due to the assumptions made for the Monte-Carlo simulation: firstly, we restricted the modelling to linear Gaussian optics (to the paraxial optical space). With linear optics we can deal with simple calculation formulae based on our pseudophakic model eye with 5 refractive spherical surfaces, but we ignore the exact shape (e.g. asphericity of both lens surfaces), the effect of the aperture, as well as the effects of decentration and tilt of optical components. Also, we positioned the thin lens IOL as well as the thick lens IOL haptic plane at the equator plane of the crystalline lens, but there might be more sophisticated strategies (Olsen & Hoffmann, 2014)

for predicting the exact anatomical IOL plane in the pseudophakic eye. As the exact design of the lens optic edge is still undisclosed for almost all lenses on the market, we have made the simplification that the IOL haptic plane coincides with the optic edge plane. However, in case of a haptic angulation or a step vault maintaining the  $360^\circ$  circular sharp optic edge this simplification might be invalid. Furthermore, in our modelling we used a preset refractive index for the IOL ( $n_L=1.52$ ) and simplified to 2 situations (preset LT and preset ET) to show the principal differences between both setups. And last but not least, we assumed that the labelled IOL power refers to the equivalent power of the IOL which is referenced to the image-side principal plane according to the ISO standard, but we are aware that measurements of IOL power at the final quality check at the IOL manufacturer's optics laboratory may differ. However, in general, most of these limitations (except the restriction to linear Gaussian optics) could easily be overcome if we know the exact shape data of the IOL for all power steps.

In conclusion, this study describes the results of a Monte-Carlo simulation based on a large data set of biometric measurements from a modern optical biometer, using linear Gaussian optics strategies to investigate the effect on the spherical equivalent refraction and ocular magnification of modelling the IOL as a thick lens rather than as a thin lens. We found that using a more realistic thick lens model for the IOL (with Coddington factor in a range  $-1.0$  to  $1.0$ ) instead of a thin lens model (with identical IOL power and axial position) resulted in a change of up to  $\pm 1.5\text{ dpt}$  in the spectacle refraction, whereas the change in ocular magnification resulting from the use of the thick lens model was small and can be ignored for clinical purposes.

## ACKNOWLEDGEMENT

The authors confirm that they do not have any financial or proprietary interest in the material or results presented in this manuscript. Open Access funding enabled and organized by Projekt DEAL.

## ORCID

Achim Langenbucher  <https://orcid.org/0000-0001-9175-6177>

Nóra Szentmáry  <https://orcid.org/0000-0001-8019-1481>

Jascha Wendelstein  <https://orcid.org/0000-0003-4145-2559>

<https://orcid.org/0000-0003-4145-2559>

<https://orcid.org/0000-0003-4145-2559>

<https://orcid.org/0000-0003-4145-2559>

## REFERENCES

- Debellemanière, G., Dubois, M., Gauvin, M., Wallerstein, A., Brenner, L.F., Rampat, R. et al. (2021) The PEARL-DGS formula: the development of an open-source machine learning-based thick IOL calculation formula. *American Journal of Ophthalmology*, 232, 58–69. Available from: <https://doi.org/10.1016/j.ajo.2021.05.004>
- Fişuş, A.D., Hirschall, N.D. & Findl, O. (2021) Comparison of 2 swept-source optical coherence tomography-based biometry devices. *Journal of Cataract and Refractive Surgery*, 47(1), 87–92. Available from: <https://doi.org/10.1097/j.jcrs.00000000000000373>
- Fyodorov, S.N., Galin, M.A. & Linksz, A. (1975) Calculation of the optical power of intraocular lenses. *Investigative Ophthalmology*, 14, 625–628.

- Gatinel, D., Debellemanière, G., Saad, A., Dubois, M. & Rampat, R. (2021) Determining the theoretical effective lens position of thick intraocular lenses for machine learning-based IOL power calculation and simulation. *Translational Vision Science & Technology*, 10(4), 27. Available from: <https://doi.org/10.1167/tvst.10.4.27>
- Gernet H, Ostholt H & Werner H (1970) Die präoperative Berechnung intraocularer Binkhorst-Linsen. 122. Vers. d. Ver. Rhein.-Westfäl. Augenärzte. Balve, Verlag Zimmermann, Germany, pp. 54-55.
- Haigis, W., Lege, B., Miller, N. & Schneider, B. (2000) Comparison of immersion ultrasound biometry and partial coherence interferometry for intraocular lens calculation according to Haigis. *Graefes Archive for Clinical and Experimental Ophthalmology*, 238(9), 765–773. Available from: <https://doi.org/10.1007/s004170000188>
- Harris, W.F. (2000) Interconverting the matrix and principal-meridional representations of dioptric power and reduced vergence. *Ophthalmic & Physiological Optics*, 20(6), 494–500.
- Hoffer, K.J. (1993) The Hoffer Q formula: a comparison of theoretic and regression formulas. *Journal of Cataract and Refractive Surgery*, 19(6), 700–712. Available from: [https://doi.org/10.1016/s0886-3350\(13\)80338-0](https://doi.org/10.1016/s0886-3350(13)80338-0)
- Hoffer, K.J. & Savini, G. (2021) Update on intraocular lens power calculation study protocols: the better way to design and report clinical trials. *Ophthalmology*, 128(11), e115–e120. Available from: <https://doi.org/10.1016/j.ophtha.2020.07.005>
- Holladay, J.T., Prager, T.C., Chandler, T.Y., Musgrove, K.H., Lewis, J.W. & Ruiz, R.S. (1988) A three-part system for refining intraocular lens power calculations. *Journal of Cataract and Refractive Surgery*, 14(1), 17–24. Available from: [https://doi.org/10.1016/s0886-3350\(88\)80059-2](https://doi.org/10.1016/s0886-3350(88)80059-2)
- Langenbacher, A., Hoffmann, P., Cayless, A., Gatinel, D., Debellemanière, G., Wendelstein, J. et al. (2022) Considerations of a thick lens formula for intraocular lens power calculation. *Zeitschrift für Medizinische Physik* S0939-3889(22)00124-6. Available from: <https://doi.org/10.1016/j.zemedi.2022.11.007>
- Langenbacher, A., Szentmáry, N., Cayless, A., Weisensee, J., Fabian, E., Wendelstein, J. et al. (2021) Considerations on the Castrop formula for calculation of intraocular lens power. *PLoS One*, 16(6), e0252102. Available from: <https://doi.org/10.1371/journal.pone.0252102>
- Langenbacher, A., Szentmáry, N., Cayless, A., Wendelstein, J. & Hoffmann, P. (2022b) Prediction of ocular magnification and aniseikonia after cataract surgery. *Acta Ophthalmologica*, 100(8), e1675–e1684. Available from: <https://doi.org/10.1111/aos.15190>
- Langenbacher, A., Szentmáry, N., Cayless, A., Wendelstein, J. & Hoffmann, P. (2022c) Prediction of the axial lens position after cataract surgery using deep learning algorithms and multilinear regression. *Acta Ophthalmologica*, 100(7), e1378–e1384. Available from: <https://doi.org/10.1111/aos.15108>
- Liou, H.L. & Brennan, N.A. (1997) Anatomically accurate, finite model eye for optical modelling. *Journal of the Optical Society of America. A, Optics, Image Science, and Vision*, 14(8), 1684–1695. Available from: <https://doi.org/10.1364/josaa.14.001684>
- Melles, R.B., Kane, J.X., Olsen, T. & Chang, W.J. (2019) Update on intraocular lens calculation formulae. *Ophthalmology*, 126(9), 1334–1335. Available from: <https://doi.org/10.1016/j.ophtha.2019.04.011>
- Norrby, N.E. & Koranyi, G. (1997) Prediction of intraocular lens power using the lens haptic plane concept. *Journal of Cataract and Refractive Surgery*, 23(2), 254–259. Available from: [https://doi.org/10.1016/s0886-3350\(97\)80350-1](https://doi.org/10.1016/s0886-3350(97)80350-1)
- Olsen, T. (2007) Calculation of intraocular lens power: a review. *Acta Ophthalmologica Scandinavica*, 85(5), 472–485. Available from: <https://doi.org/10.1111/j.1600-0420.2007.00879.x>
- Olsen, T., Cooke, D.L., Findl, O., Gatinel, D., Koch, D., Langenbacher, A. et al. (2023) Surgeons need to know more about IOL design for accurate power calculation. *Journal of Cataract and Refractive Surgery*. Available from: <https://doi.org/10.1097/j.jcrs.00000000001159> Publish Ahead of Print.
- Olsen, T., Corydon, L. & Gimbel, H. (1995) Intraocular lens power calculation with an improved anterior chamber depth prediction algorithm. *Journal of Cataract and Refractive Surgery*, 21(3), 313–319. Available from: [https://doi.org/10.1016/s0886-3350\(13\)80140-x](https://doi.org/10.1016/s0886-3350(13)80140-x)
- Olsen, T. & Hoffmann, P. (2014) C constant: new concept for ray tracing-assisted intraocular lens power calculation. *Journal of Cataract and Refractive Surgery*, 40(5), 764–773. Available from: <https://doi.org/10.1016/j.jcrs.2013.10.037>
- Olsen, T.J. (2006) Prediction of the effective postoperative (intraocular lens) anterior chamber depth. *Journal of Cataract and Refractive Surgery*, 32(3), 419–424. Available from: <https://doi.org/10.1016/j.jcrs.2005.12.139>
- Retzlaff, J.A., Sanders, D.R. & Kraff, M.C. (1990) Development of the SRK/T intraocular lens implant power calculation formula. *Journal of Cataract and Refractive Surgery*, 16(3), 333–340. Available from: [https://doi.org/10.1016/s0886-3350\(13\)80705-5](https://doi.org/10.1016/s0886-3350(13)80705-5)
- Sanders, D.R., Retzlaff, J.A., Kraff, M.C., Gimbel, H.V. & Raanan, M.G. (1990) Comparison of the SRK/T formula and other theoretical and regression formulas. *Journal of Cataract and Refractive Surgery*, 16(3), 341–346. Available from: [https://doi.org/10.1016/s0886-3350\(13\)80706-7](https://doi.org/10.1016/s0886-3350(13)80706-7)
- Savini, G., Taroni, L. & Hoffer, K.J. (2020) Recent developments in intraocular lens power calculation methods-update 2020. *Annals of Translational Medicine*, 8(22), 1553. Available from: <https://doi.org/10.21037/atm-20-2290>
- Shammas, H.J. (2004) *Intraocular lens power calculations*. USA: Slack Inc. ISBN-13: 978-1556426520.
- Simpson, M.J. (2021) Pre-clinical estimation of the intraocular lens A-constant, and its relationship to power, shape factor, and asphericity. *Applied Optics*, 60(19), 5662–5668. Available from: <https://doi.org/10.1364/AO.426155>
- Wendelstein, J.A., Reifeltshammer, S.A., Hoffmann, P.C., Fischinger, I., Mariacher, S., Bolz, M. et al. (2022) Project hyperopic power prediction: accuracy of 13 different concepts for intraocular lens calculation in short eyes. *The British Journal of Ophthalmology*, 106(6), 795–801. Available from: <https://doi.org/10.1136/bjophthalmol-2020-318272>

**How to cite this article:** Langenbacher, A., Szentmáry, N., Cayless, A., Gatinel, D., Debellemanière, G., Wendelstein, J. et al. (2024) Monte-Carlo simulation of a thick lens IOL power calculation. *Acta Ophthalmologica*, 102, e42–e52. Available from: <https://doi.org/10.1111/aos.15666>